Preprints, 17th Conf. on Hurricanes & Tropical Meteorology, AMS, Miami, Apr. 7-10, 1987, 347-350.

13A.4

THREE-DIMENSIONAL STRUCTURE OF THE EYEWALL OF HURRICANE NORBERT AS DETERMINED FROM AN AIRBORNE DOPPLER RADAR

Frank D. Marks, Jr.
Hurricane Research Division, NOAA/AOML
4301 Rickenbacker Causeway
Miami, FL 33149

and

Robert A. Houze, Jr.
Department of Atmospheric Science
University of Washington
Seattle, Washington 98195

1. INTRODUCTION

On 24-25 September 1984 a dedicated experiment to study the water transport within the region surrounding the eyewall of Hurricane Norbert was carried out using the two NOAA WP-3D research aircraft. One aircraft equipped with the airborne Doppler radar flew repeated radial penetrations in and out of the eyewall with 90 deg turns in the eye at 3 km altitude (Fig. 1). The resultant "L-shaped" patterns were flown to facilitate good dual-Doppler coverage in each quadrant of the eyewall region out to a radius of 40 km from the storm center. The second aircraft, at 6 km altitude, flew repeated radial penetrations in and out of the eyewall sampling the hydrometeor distributions in different quadrants of the storm.

This paper concentrates on the structure of the three dimensional wind field as derived from the airborne Doppler measurements and how this wind structure relates to storm movement. In particular, the procedure used to compute the environmental wind and the vortex perturbation wind will be outlined.

2. STORM STRUCTURE

This study covers the period 0018-0215 GMT 25 September 1986. At this time Hurricane Norbert was located near 22.5°N, 112.3°W (over the eastern Pacific Ocean), approximately 260 km west-southwest of the southern tip of Baja California, and was moving northwestward at 5.6 m s^{-1}. Maximum winds at the 3 km flight level were 50-55 m s^{-1} and the central pressure was 952 mb [details of the storm history and track are given by Gunther and Cross (1985)].

Fig. 1 shows the aircraft flight track (relative to the moving storm center) and the radar structure as viewed from the lower fuselage radar on the aircraft at 3 km altitude. The storm track was determined objectively from the flight-level winds at 3 km altitude using the technique described by Willoughby and Chelmow (1982).

Fig. 1 shows that the strongest reflectivity was in a 10-15 km wide band, 20-25 km out from the storm wind center, on the west and south side of the storm. There was very little strong reflectivity (>36 dBZ) on the east and north side of the storm.

3. DATA ANALYSIS

The Doppler radar data used in this study was obtained from the airborne Doppler radar installed on the NOAA WP-3D aircraft at 3 km altitude. The radar had a wavelength of 3.2 cm, a vertical beamwidth of 1.9°, and a horizontal beamwidth of 1.35°. The antenna, located in the tail of the aircraft, pointed at right angles to the aircraft's ground track while sweeping through elevation angles of 0-360°. Thus, the Doppler radar measured the horizontal component of the precipitation particle motion perpendicular to the flight track. When the antenna was not pointing horizontally, the vertical motions of the precipitation particles also affected the measured velocity along the radar beam. When the antenna was pointing either directly upward or downward (vertical incidence), the vertical motion of particles was measured along

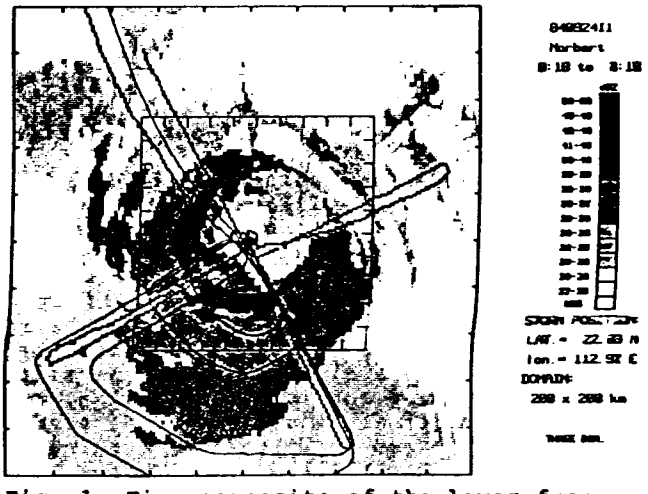

Fig. 1. Time composite of the lower fuselage radar reflectivity for 0020-0215 GMT 25 September 1984. The flight track of the aircraft at 3 km altitude is indicated by the thick solid line. The track of the second aircraft, at 6 km altitude, is indicated by the thin solid line. The reflectivity is shaded at 25, 28, 35, and 39 dBZ. The region covered by the radar composite is 200 by 200 km and the inner box is 100 km on a side. The ticks on the outer box are 20 km apart and on the inner box 10 km apart. The storm wind center is indicated by the hurricane symbol.

the beam. The antenna rotated at a rate of one revolution per 7.5 s which provided data at all elevation angles once every 0.8 km of flight track.

The three-dimensional wind field within 40 km of the storm center was derived from a dual-Doppler analyses in each quadrant of the storm. Each flight leg used in the dual Doppler analysis was approximately 75 km long and took 10 min of flight time. The airborne Doppler data extended 40 km out from the radar. Hence, only the inner 40 km of each flight leg was used for the dual Doppler analysis. This choice of a 40 km maximum dimension resulted in a maximum time separation between Doppler radial velocities from the two legs of 12 min.

The horizontal wind field in three-dimensions was determined using the technique first described by Jorgensen et al. (1983) and as modified by Marks and Houze (1987). The vertical wind components were derived by integrating the continuity equation using the divergence computed from the horizontal wind field.

The Doppler-derived wind fields for the four quadrants were combined to form a storm composite wind field 75 x 75 km on a side, centered on the storm circulation center, extending from 0.5-12.0 km in altitude. Any holes in the composite wind field, caused by missing Doppler wind estimates (i.e., a missing wind component from one of the legs in an L-shaped pattern), were filled using an iterative filling and filtering scheme. This scheme employed a modification of the Storm Centered Analysis ALgorithm (SCAAL) described by Willoughby, et al. (1984), designed to work with the composite wind analysis rather than flight level data. The mean vortex and the wave number one and two asymmetries from the SCAAL fit to the composite wind analysis were used to initially fill the holes. The composite analysis was then matched to the filled values with a multi-pass filtering scheme.

The filter, designed by Leise (1981), was applied to the filled winds a number of times, with the short wave cutoff decreasing each time the filter was applied (e.g. $8\Delta x$ on the first pass, $4\Delta x$ on the second pass, and $2\Delta x$ on the last pass). After each filter application the original composite wind values were inserted back into the filtered wind analysis. Hence, the filter was only being applied to the holes, and not the original winds. The final step in the process was to filter the original winds and the filtered winds in the holes with a $2\Delta x$ cutoff.

The reflectivity value at each point in the wind analysis was checked, and the wind values with corresponding reflectivity values <1 dBZ were deleted to prevent the filter/filling process from generating circulations where we had no scatterers. Divergence and vertical velocity was recomputed for each point in the domain that had a wind.

4. THREE-DIMENSIONAL WIND STRUCTURE

The three-dimensional wind structure of the inner-core of the vortex was described by partitioning the wind field into three components: (1) the mean vortex; (2) the environmental flow; and (3) a perturbation wind. The wind partitioning is defined as

$$V(r,\lambda,z) = V_e(z) + V_s(r,z) + V'(r,\lambda,z) \quad (1)$$

where V is the observed wind as a function of radius (r), azimuth (λ), and height (z), V_e is the environmental wind as a function of z only, V_s is the mean vortex (a function of r and z only), and V' is the perturbation wind as a function of r, λ, and z. The mean vortex (V_s), shown in Fig. 2, is defined as

$$V_s(r,z) = 1/2\pi \int_0^{2\pi} V(r,\lambda,z)\, d\lambda. \quad (2)$$

V_s can be separated into two components, the tangential and radial wind.

As can be seen in Fig. 2, there is a tangential wind maximum of 52 m s^{-1}, centered at 26 km radius (~4 km radially outward from the reflectivity maximum). This tangential wind maximum is relatively shallow in vertical extent, and has a gradual slope radially outward with increasing height.

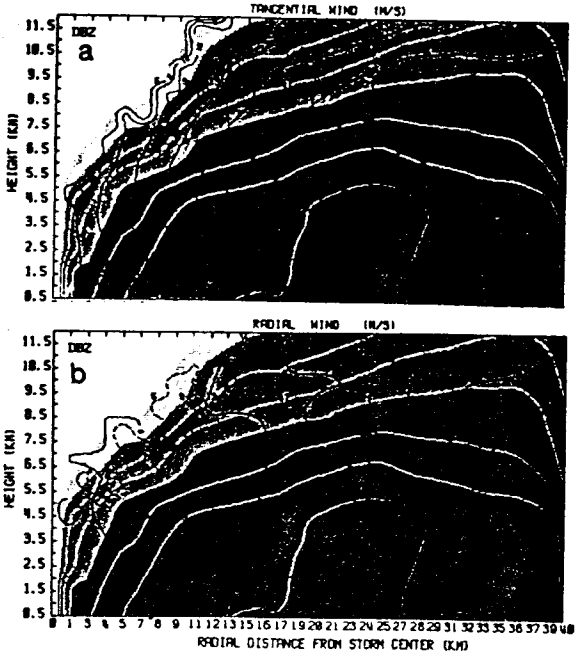

Fig. 2. Radius-height cross-sections of the mean airborne Doppler derived winds and tail radar reflectivity for the mean vortex (V_s): (a) mean tangential wind component (m s^{-1}) and reflectivity (dBZ); and (b) mean radial wind component (m s^{-1}) and reflectivity (dBZ). Reflectivity values are depicted by shades of gray and the wind components by contour lines. Positive values are indicated by solid lines and negative values by dashed lines.

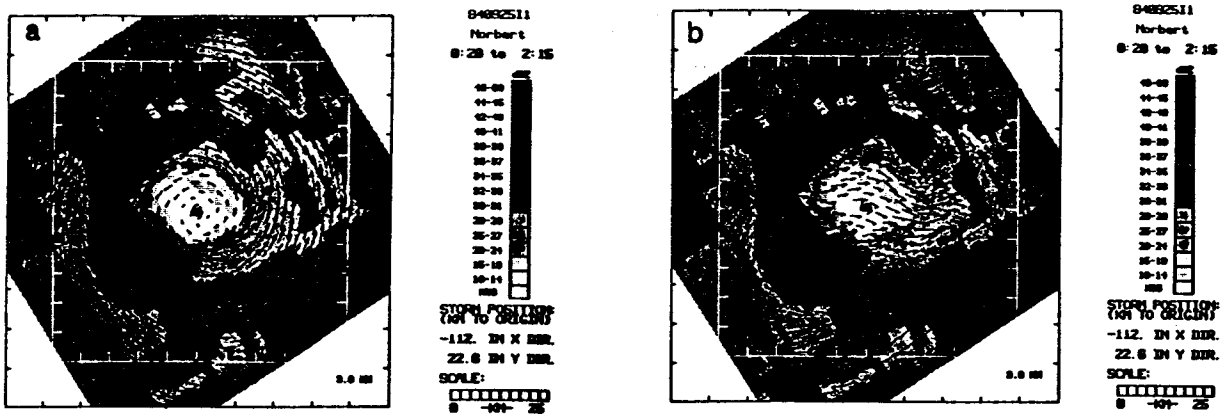

Fig. 3. Time composites of the tail radar reflectivity and the airborne Doppler-derived winds at 3 km altitude for 0020-0215 GMT 25 September 1984. The analysis covers the region of the storm enclosed in the inner box in Fig. 1. The analysis domain is 100 km on a side and the tick marks are 10 km apart. The reflectivity is shaded at 10, 20, 30 and 36 dBZ. Superimposed over the reflectivity field in (a) is the total wind field (V), and in (b) the perturbation wind field (V'). The length of the arrows indicate the strength of the wind, where the arrow lengths in (b) have been multiplied by a factor of 4.5. The storm wind center is indicated by the hurricane symbol.

The radial wind has weak outflow over most of the inner core, with peak outflow of 4-5 m s^{-1} above 10 km, from 25 km radius outward. There is a narrow band of outflow of 4 m s^{-1} inside the tangential wind maximum centered at 15-20 km radius, and the radial flow is weakly inward above 3 km inside 15 km radius.

Given the mean vortex (V_s), the environmental wind (V_e) and the perturbation wind (V') may be approximated as

$$V(r,\lambda,z) - V_s(r,z) = V_e(z) + V'(r,\lambda,z). \quad (3)$$

There is no a priori solution for V_e from (3). Hence, we must make a hypothesis about the structure of V_e or V' and check our hypothesis a posteriori against available synoptic data.

The hypothesis used was that V_e is defined as the areal average of the LHS of (3), or

$$V_e(z) = 1/A \iint_A (V - V_s)\, dA, \quad (4)$$

where A is the area covered by the analysis domain (75 x 75 km). This hypothesis is equivalent to assuming that the areal average of V' over the analysis domain is zero, or that the perturbation wind field is symmetric about the vortex (i.e., the vortex perturbation). Hence, if no other circulations are present then V_e is all that is left.

Fig. 3 shows the V and V' field at the 3 km altitude. The V' field shows a wave number one cyclonic/anticyclonic eddy couplet centered at the radius of maximum wind (~25 km), with a cyclonic eddy 90° to the right of the storm track (323°/143° axis), and an anticyclonic eddy 90° to the left of the track. The eddy pattern is present in the V' field at all analysis levels from 0.5-12.0 km. These eddies are similar in structure and orientation to those observed in recent analytical and numerical studies of storm motion (Willoughby, personal communication), and are probably a result of the movement of the storm through the environment. [The eddy pattern also points up the way the storm moves, i.e., the mean vortex advects the perturbation cyclonic vorticity associated with the cyclonic eddy towards the direction of motion, and advects the perturbation anticyclonic vorticity to the rear of the storm].

Because V' is dominated by this symmetric perturbation associated with the vortex, it seems reasonable to assume that the areal average of V' = 0. Hence, it seems reasonable to estimate V_e by (4).

Fig. 4 shows a hodograph of V_e computed using (4). V_e is northwesterly below 3 km, changing to increasing south, south-

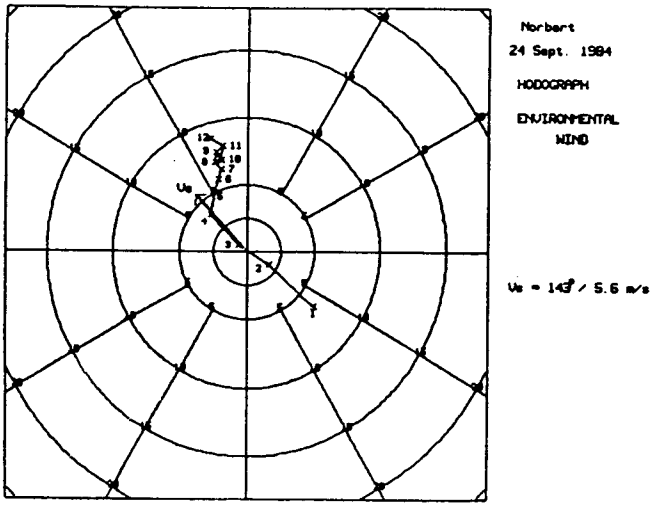

Fig. 4. Hodograph of the estimated environmental wind (V_e) derived from the Doppler wind analysis. Numbers with small crosses indicate V_e at 1 km altitude intervals. The solid arrow indicates the speed and direction of the storm motion (V_s).

easterly flow aloft. From 4.0-7.0 km altitude, V_e is of the same magnitude as the storm motion (V_s) and slightly to the right of the track. This V_e profile computed from the Doppler analysis is in good qualitative agreement with the large-scale synoptic analysis (not shown). At the gradient wind level (~1.5 km) there was weak northwesterly flow coming down the coast of Baja California. At the 200 mb level (~9-10 km) the flow was southerly as a trough approached the coast from the west (Gunther and Cross, 1985).

5. ACKNOWLEDGMENTS

The author appreciates the commitment of the NOAA aircraft to this project and Dr. Robert Burpee's expert field program coordination, which led to the highly successful investigation of Hurricane Norbert.

REFERENCES

Gunther, E.B., and R.L. Cross, 1985: Eastern North Pacific Tropical Cyclones of 1984. Mon. Wea. Rev., 113,1393-1410.

Jorgensen, D.P., P.H. Hildebrand, and C.L. Frusch, 1983: Feasibility test of an airborne pulse-Doppler meteorological radar. J. Climate Appl. Meteor., 22, 744-757.

Leise, J.A., 1981: A multi-dimensional scale-telescoped filter and data extension package. NOAA Tech. Memo. ERL-WPL-82, Boulder, CO, 20 pp.

Marks, F.D, Jr., and R.A. Houze, Jr., 1987: Inner core structure of Hurricane Alicia from airborne Doppler radar observations. accepted by J. Atmos. Sci.

Willoughby, H.E., and M.B. Chelmow, 1982: Objective determination of hurricane tracks from aircraft observations. Mon. Wea. Rev., 110, 1298-1305.

Willoughby, H.E., F.D. Marks, Jr., and R.J. Feinberg, 1984b: Stationary and propagating convective bands in asymmetric hurricanes. J. Atmos. Sci., 41, 3189-3211.